Supplementary Information

High-performance tungsten carbide electrocatalysts for Hydrogen Evolution Reaction

Jingwen Huang, Jing Li , Wenting Hong , Bao Wang*, and Wei Liu*

E-mail: baowang@ipe.ac.cn，liuw@fjirsm.ac.cn

Experimental Section

Oxidation of W foil: W foil is ultrasonically cleaned in acetone, ethanol, and distilled water for 15 minutes in sequence. The cleaned W foil is dried in an oven at 100℃. The dried W foil is calcined in air at 600℃ for 2 h in the tube furnace with a ramping rate of 10℃ per min to form WO_2 on the surface of the W foil. Then WO_2/W film is cooled by natural air convection in the furnace back to the ambient condition. Finally, the pre-treated WO_2/W film is placed on an alumina boat, the reactions are performed at the temperature of 800℃for 40 min in rough vacuum in order to form WO_3/W.

Preparation of WC/W electrocatalyst: To prepare the WC/W sample, the WO_3/W film is heated up to 800℃ with a flowing mixture of H_2 and Ar (H_2/Ar=30:70) at a heating rate of 20℃ per min, then the CH_4 (15 sccm) gas is inlet into the tube to make WO_3/W film to undergo carburization in a gas flow of 13 vol% CH_4 /26 vol% H_2/61vol% Ar in a tubular furnace at 800 °C for 20 min. After the carburization process, the methane is turned off, the sample is heated to 900℃ in an Ar gas flow of

200 sccm and undergoes hydrogen treatment at 900℃ for 30 min. At last, generated WC/W film cools down to the room temperature in an atmosphere of argon.

Structural characterizations of the electrocatalyst.

The morphology of the as-grown WO_{3-x}, WO_3, and WC samples was characterized by scanning electron microscopy (HITACHI UHR FE-SEM SU8010). X-ray diffraction (XRD) spectra were obtained using the D8 ADVANCE diffractometer with Cu Kα radiation (λ = 1.5418 Å). X-ray photoelectron spectroscopy (XPS) measurements are carried out by a ESCALAB 250Xi system (Thermo Fisher), equipped with a 100 W Al Kα source on a spot size of 100 μm at a 45° incident angle. The binding energy scan ranges from 0 to 1200 eV with an interval step of 1 eV, high-intensity excitation is provided by monochromatic Al Ka X-rays that are 1486.6 eV in energy with a 0.48 eV resolution at full width at half-maximum. The binding energy scale is calibrated to carbon line of 284.8 eV. All XPS spectra are recorded with a resolution of 50 meV. Each data set is first corrected for the nonlinear emission background. The data is then fitted with Gaussian function to find the deconvoluted peak positions. Transmission electron microscopy (TEM), high-resolution TEM (HRTEM), selected-area electron diffraction (SAED) and energy dispersive X-ray spectroscopy (EDS) mapping studies are conducted on a probe-corrected transmission electron microscope operating at 200 kV (FEI Titan F20 TEM).

Electrochemical performance measurement

All electrochemical measurements were performed on a CHI 660e electrochemical workstation with a standard three-electrode cell in the electrolyte of 0.5 mol/L H_2SO_4 (pH = 0) and 1 mol/L KOH (pH = 14), respectively. The samples can be directly used as working electrode without other treatment, the saturated calomel electrode (SCE) is used as reference electrode and platinum wire is used as counter electrode. The polarization curves were obtained by linear sweep voltammograms scan from 0 to -0.5 V (vs. Ag/AgCl) with a sweep rate of 2 mV • s^{-1} Electrochemical impedance spectroscopy (EIS) measurements were conducted over a frequency range from 1000 Hz to 0.01 Hz. The stability was tested by cyclic voltammetry under the acid and basic media at potentials between 0 V and -0.6 V at a scan rate of 100 mV/s and a sweep segment of 4000.

Table S1 Comparison of HER performance of WC/W with other tungsten carbide electrocatalysts

Materials	Electrolyte	η_{onset} (mV)	η_{10} (mV)	Tafel slope (mV/dec)	Ref.
WC/W	**0.5 M H_2SO_4**	**30**	**87**	**55.5**	**This work**
	1 M KOH	**22**	**68**	**38.89**	
WC/W_2C heterojunction	0.5 M H_2SO_4	~	69	52	Ref. S1
	1 M KOH	~	56	59	
WC-CNTs	0.5 M H_2SO_4	15	145	72	Ref. 43
	1 M KOH	16	137	106	
p-WC xNWs/CC	0.5 M H_2SO_4	39	118	55	Ref. 36
	1 M KOH	56	122	56	
TCNC spheres	0.5 M H_2SO_4	~	290	110	Ref. 19
	1 M KOH	~	300	133	
2D i-WC-G	0.5 M H_2SO_4	~	120	38	Ref. S2
	1 M KOH	~	225	108	
W_2C@CNT-S	0.5 M H_2SO_4	60	176	57.4	Ref. S3
	1 M KOH	40	148	56.2	
CoW/CN	1 M KOH	31	98	125	Ref. S4
W_xC@WS_2	0.5 M H_2SO_4	70.3	146	61	Ref. S5
W_2C/MWNT	0.5 M H_2SO_4	50	123	45	Ref. 15
WC nanoparticles	0.5 M H_2SO_4	~	125	84	Ref. 30
Ni/WC	0.5 M H_2SO_4	~	53	43.5	Ref. S6
3%Pt/WC/C_{10}	0.5 M H_2SO_4	~	85	85	Ref. S7
α-W_2C/WN@G	0.5 M H_2SO_4	~	120	68.6	Ref. 14
MoS_2/WC/RGO	0.5 M H_2SO_4	~	200	41	Ref. S8
WC nanoparticles	0.5 M H_2SO_4	~	200	~	Ref. S9
WC bulk	0.5 M H_2SO_4	~	150	~	Ref. S10
W_2C-HS	0.5 M H_2SO_4	~	153	67.8	Ref. S11
W_2C-WP@NC	0.5 M H_2SO_4	~	83	61	Ref. S12

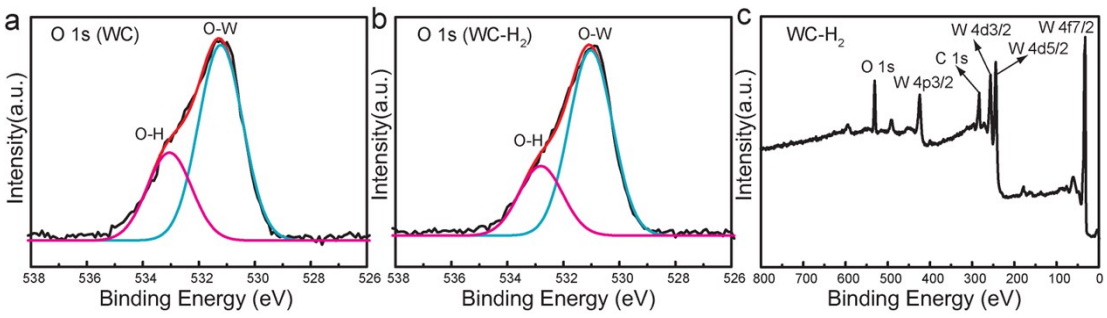

Figure S1. X-ray photoelectron spectroscopy (XPS) spectra of O 1s of (a) WC and (b) WC-H_2. (c) X-ray photoelectron spectroscopy (XPS) full spectra of WC-H_2.

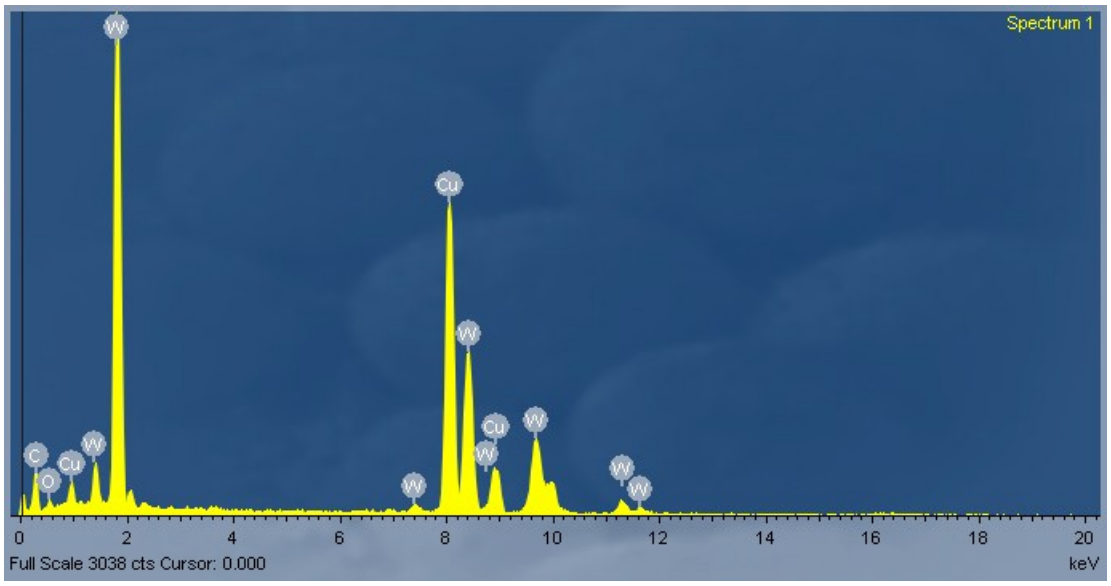

Figure S2. EDS analysis on the chemical composition of WC.

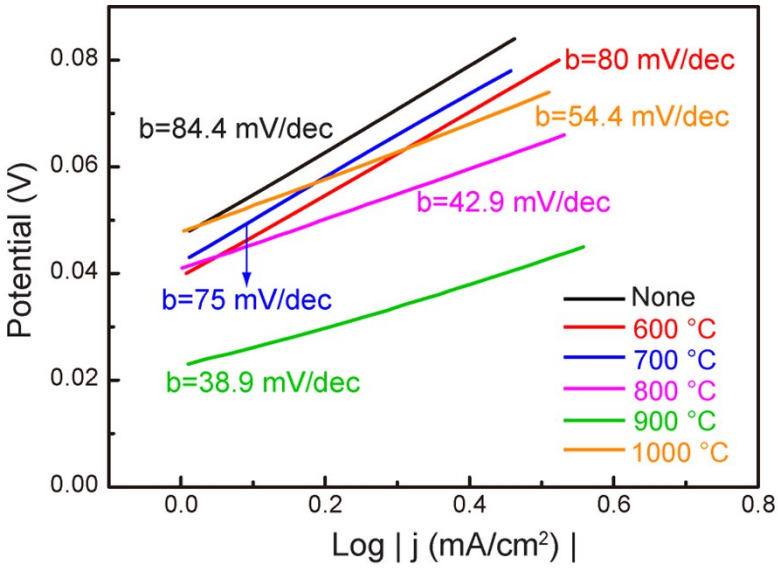

Figure S3. The Tafel plots of $WC(WO_3)$ catalysts hydrogen-treated at different temperature measured in 1 M KOH solution.

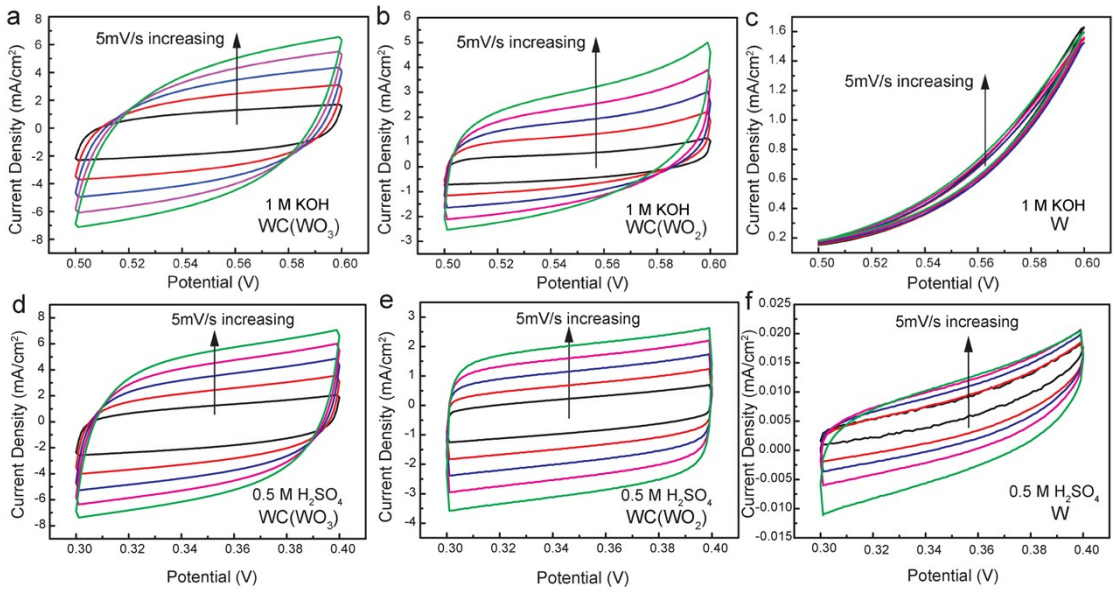

Figure S4. Double-layer capacitance (C_{dl}) measurements of (a) $WC(WO_3)$, (b) $WC(WO_2)$, and (c) W catalyst by taking advantage of electrochemical cyclic voltammogram in 1 M KOH. The scan speeds are set in the range of 5 to 25 mV/s with an interval of 5 mV/s.

C_{dl} can be extracted from the slope of the fitted lines of the plots in the figure of Δj

against the cyclic voltammetry scan rates, where Δj is derived by subtracting the negative current density from the positive current density (j_a-j_c) at a given potential of 0.55 V versus RHE. Double-layer capacitance (C_{dl}) measurements of (d) WC(WO_3), (e) WC(WO_2), and (f) W catalyst by taking advantage of electrochemical cyclic voltammogram in 0.5 M H_2SO_4. The scan speeds are set in the range of 5 to 25 mV/s with an interval of 5 mV/s. C_{dl} can be extracted from the slope of the fitted lines of the plots in the figure of Δj against the cyclic voltammetry scan rates, where Δj is derived by subtracting the negative current density from the positive current density (j_a-j_c) at a given potential of 0.35 V versus RHE.

To calculate the per-site turnover frequency (TOF), we used the following formula[39]:

$$TOF = \frac{(3.12 \times 10^{15} \frac{H_2/s}{cm^2} per \frac{mA}{cm^2}) \times |j|}{No.\ of\ active\ sites \times A_{ECSA}}$$

$$No.\ of\ active\ sites(WC) = \left(\frac{2\ atoms/unit\ cell}{21.04\dot{A}^3/unit\ cell}\right)^{\frac{2}{3}} = 2.08 \times 10^{15}$$

$$A_{ECSA}^{WC(WO_3)} = \frac{2 \times C_{dl_{(WC(WO_3))}}\ mF\ cm^{-2}}{40\ \mu F\ cm^{-2} per\ cm^2_{ECSA}}$$

$$A_{ECSA}^{WC(WO_2)} = \frac{2 \times C_{dl_{(WC(WO_2))}}\ mF\ cm^2}{40 \mu F\ cm^2 per\ cm^2_{ECSA}}$$

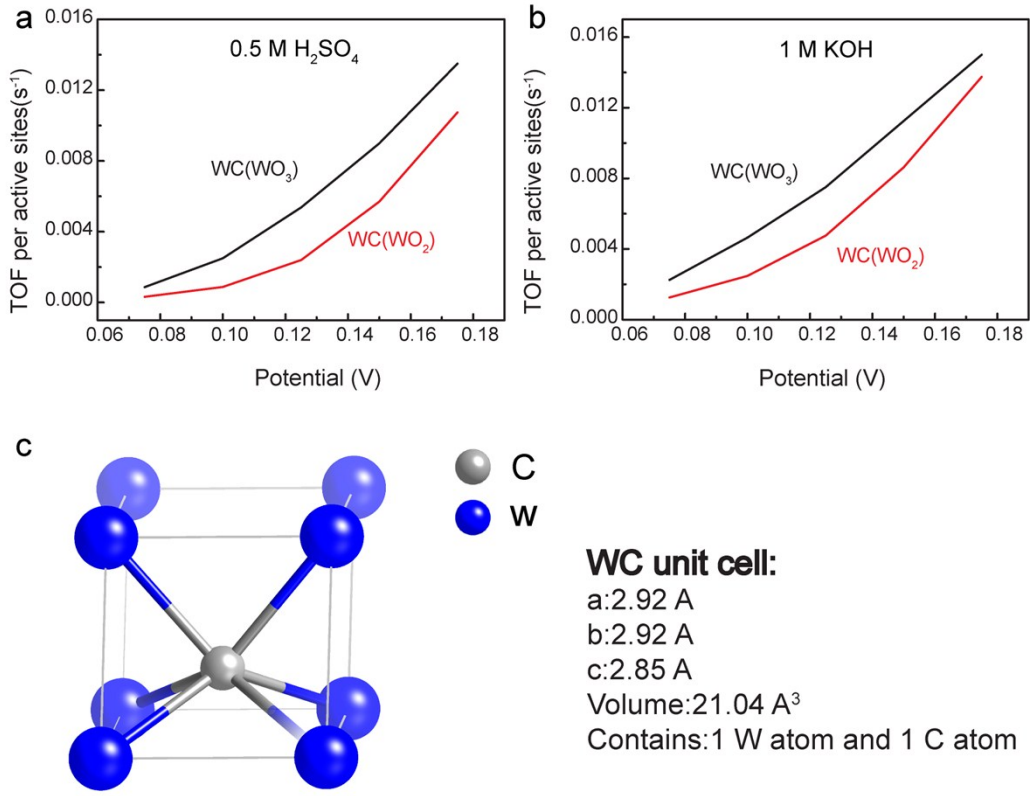

Figure S5. TOF values of $WC(WO_3)$ and $WC(WO_2)$ using 40 μF cm^{-2} as the specific capacitance standard in (a) 0.5 M H_2SO_4 solution and (b) 1 M KOH solution. (c) WC unit cell. W atoms: blue and C atoms: grey.

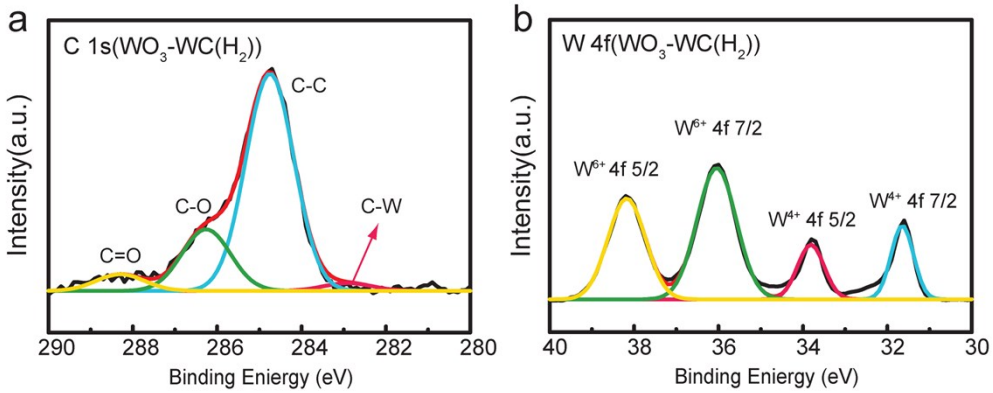

Figure S6. X-ray photoelectron spectroscopy (XPS) spectra of (a) C 1s and (b) W 4f of WC after the stability test in 1 M KOH solution.

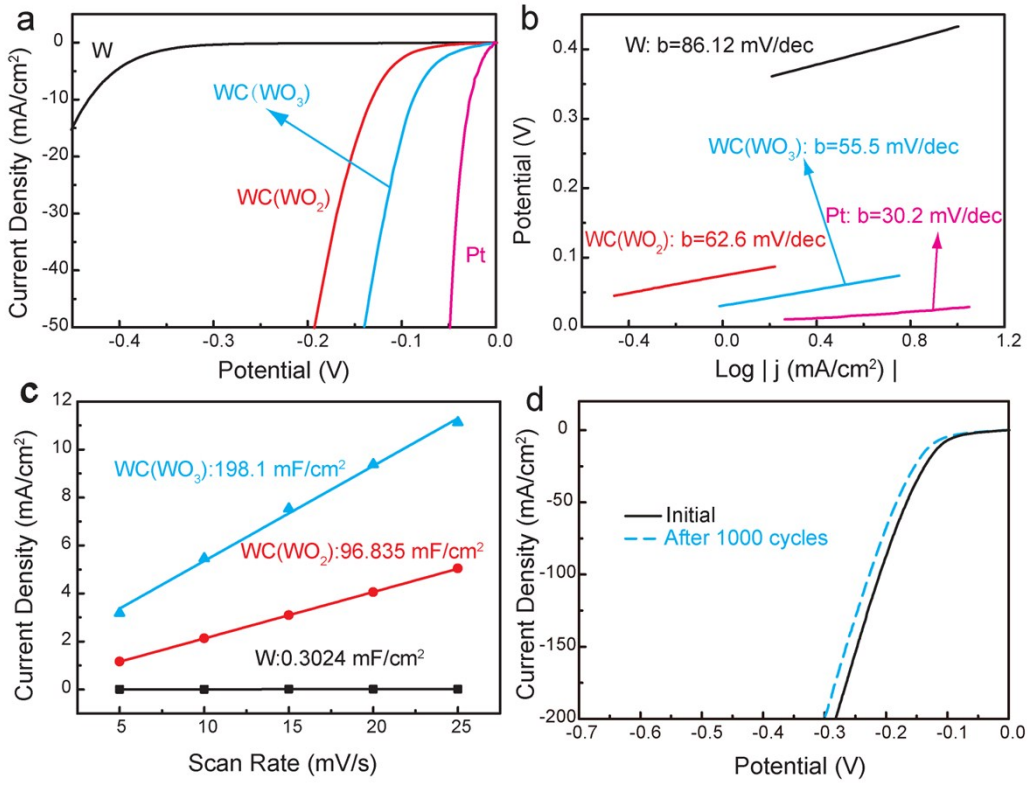

Figure S7. (a) Polarization curves of W, $WC(WO_2)$, $WC(WO_3)$ and commercial Pt/C catalysts measured in 0.5 M H_2SO_4 solution. (b) The corresponding Tafel plots. (c) Current density variation at a given potential of 0.35 V vs RHE plotted against scan rate fitted to a linear regression enables the C_{dl} estimation. (d) Polarization curves recorded from $WC(WO_3)$ before and after 1000 cycles of cyclic voltammetry test at a scan rate of 0.1 V/s in 0.5 M H_2SO_4.

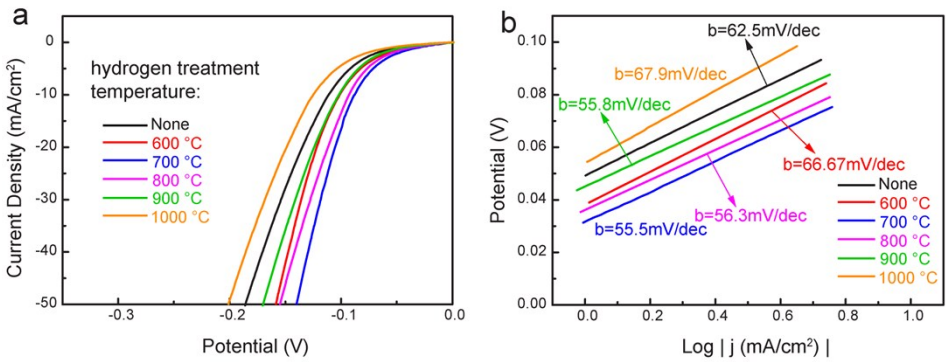

Figure S8. (a) Polarization curves of $WC(WO_3)$catalysts hydrogen-treated at different temperature measured in 0.5 M H_2SO_4 solution. (b) The corresponding Tafel plots.

REFERENCES

[S1] L. Zhang, Y. Ma, Z. Lang, Y. Wang, S. U. Khan, G. Yan, H. Tan, H. Zang and Y. Li. *J. Mater. Chem. A*, 2018. **6**. 15395-15403.

[S2] M. Zenga, Y. Chena, J. Lia, H. Xuea, R. G. Mendesb, J. Liua, T. Zhanga, M. H. Rümmeli, L. Fu, *Nano Energy*, 2017, **33,** 356-362.

[S3] Y. Hu, B. Yu, W. Li, M. Ramadoss and Y. Chen, *Nanoscale*, 2019, **11**, 4876-4884.

[S4] H. Jin, J. Chen, S. Mao, and Y. Wang, *Acs Appl Mater Inter*., 2018, **10,** 22094-22101.

[S5] F. Wang, P. He, Y. Li, T. A. Shifa, Y. Deng, K. Liu, Q. Wang, F. Wang, Y. Wen, Z. Wang, X. Zhan, L. Sun and J. He, *Adv. Funct. Mater*., 2017, **27**, 1605802.

[S6] Y. Y. Ma, Z. L. Lang, L. K. Yan, Y. H. Wang, H. Q. Tan, K. Feng, Y. J. Xia, J. Zhong, Y. Liu, Z. H. Kang and Y. G. Li, *Energy Environ. Sci.*, 2018, **11**, 2114-2123.

[S7] X. Wei and N. Li, *Appl. Surf. Sci*., 2019, **463,** 1154-1160.

[S8] Y. Yan, B. Xia, X. Qi, H. Wang, R. Xu, J. Y. Wang, H. Zhang and X. Wang, *Chem. Commun*., 2013, **49**, 4884-4886.

[S9] S. T. Hunt, T. Nimmanwudipong and Y. R. Leshkov, *Angew. Chem. Int. Ed.,* 2014, **53**, 5131-5136.

[S10] M. C. Weidman, D. V. Esposito, Y. C. Hsu and J. G. Chen, *J Power Sources*, 2012, **202**, 11-17.

[S11] Y. Ling, F. Luo, Q. Zhang, K. Qu, L. Guo, H. Hu, Z. Yang, W. Cai, and H. Cheng, *ACS Omega*, 2019, **4**, 4185−4191.

[S12] M. Shi, W. Li, J. Fang, Z. Jiang, J. Gao, Z. Chen, F. Sun and Y. Xu, *Electrochimica Acta*., 2018, **283**, 834-841.